Proceedings of International Conference on Heat Exchanger Fouling and Cleaning - 2015 (Peer-reviewed)
June 07 - 12, 2015, Enfield (Dublin), Ireland
Editors: M.R. Malayeri, H. Müller-Steinhagen and A.P. Watkinson
Published online
www.heatexchanger-fouling.com

FOULING MANAGEMENT OF THERMAL CRACKING UNITS

E.M. Ishiyama, J. Kennedy and S.J. Pugh

IHS Energy, 133 Houndsditch, EC3A 7BX London, United Kingdom
*E-mail: Edward.ishiyama@ihs.com

ABSTRACT

Visbreakers (VB) and other thermal cracking units are thermal processes in crude oil refineries which upgrade heavy petroleum, usually residual oils produced from atmospheric or vacuum distillation of crude oil. The associated process streams of these units consist of heavy hydrocarbons with very high viscosities and impurities, resulting in fouling of the heat exchangers used to cool or heat these streams.

This manuscript presents a practical fouling analysis for thermal cracking units in a German refinery. Fouling management at this refinery was initiated as part of the refinery energy saving program. Following similar analysis of the refinery's crude pre-heat trains, heat exchanger networks associated in the thermal cracking units were modelled by entering the plant monitoring data, network topology and heat exchanger geometries to a commercial heat exchanger network simulator, SmartPM. Fouling behaviour of vacuum residue streams and thermal cracker residue streams were identified and quantified. Both chemical reaction fouling and particulate fouling mechanisms were identified to be responsible for the fouling in these streams. Dynamic fouling models were fitted and used to predict fouling of these heavy petroleum streams, which fouled on both the shell- and tube- sides of the shell-and-tube heat exchangers.

INTRODUCTION

Thermal cracking processes are used in the refinery to upgrade heavy, less valuable, hydrocarbon residues to more valuable products. A commonly used thermal cracking process is visbreaking. This is a non-catalytic thermal process aimed at reducing the viscosity of hydrocarbon residues. Visbreaking processes residues from the atmospheric or vacuum distillation columns: these are preheated through a series of heat exchangers before entering a 'visbreaking furnace'. This unit is operated at conditions selected to thermally crack the feed. There are two types of visbreaking technologies in wide use: coil visbreaking and the high soaker visbreaking. In coil visbreaking, the conversion is achieved by high-temperature cracking for a predetermined, relatively short period of time in the heater. Soaker visbreaking is a lower temperature/higher-residence-time process where the majority of conversion occurs in a reaction vessel or soaker drum. In the latter, the two-phase heater effluent is held at a lower temperature for a longer period of time.

Due to the composition of the associated streams in a visbreaking system, the heat exchangers and transport pipes are subject to severe fouling. A simplified illustration of a thermal cracking unit at the refinery is presented in Fig. 1. From Pump A, the vacuum residue (VR) stream flows through a series of heat exchangers preheating it to ~ 330 °C. The preheated VR stream enters the furnace where it is heated to ~480 °C and separated in a drum to its products. The residue from the visbreaker (VBR) is cooled down by preheating the VR stream in exchangers E1 to E4.

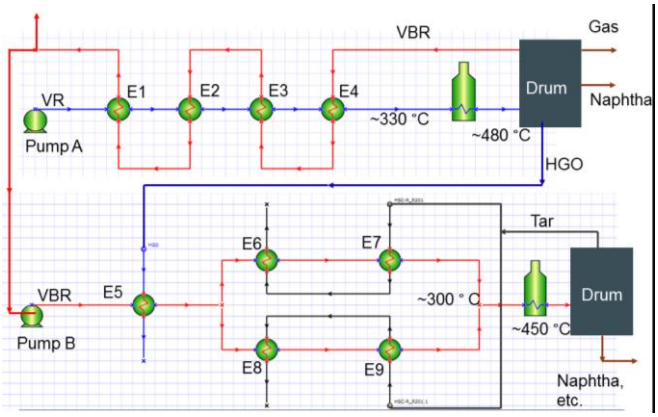

Fig. 1 Simplified illustration of thermal cracking. VR = Vacuum residue stream, VBR = Visbreaker residue stream, HGO = Heavy gas oil stream.

VR streams in industrial practice are known to be prone to fouling. Fouling rate of a mixture of VR and diluent blends were reported to increase moderately with increasing temperature in laboratory-controlled conditions (Hong and Watkinson, 2009). Furthermore, the dependence of the initial fouling rates on surface temperature was reported to fit a chemical reaction type fouling model with an Arrhenius temperature dependency. An apparent activation energy of 68 kJ mol^{-1} was reported for VR-diluent blend fouling by Hong and Watkinson (2009).

VBR streams consist of highly unstable tar by which precipitate in the visbreaker process, along with a high concentration of asphaltene particulates. These particulates

are severe fouling threats to the energy recovery system. The VBR stream experiences particulate fouling.

Particulate fouling strongly depends on the operating condition of the unit. Analyses for heat exchangers including double pipe and plate and flame units are reported by several groups (Melo and Pinheiro, 1984; Mueller-Steinhagen and Bloechl, 1988; Mueller-Steinhagen et al., 1988; Vašak et al., 1995).

The VBR stream is re-heated up to ~300 °C through a series of heat exchangers, E5 to E9, and enters a furnace where the temperature is further increased to ~ 450 °C. This second thermal cracker is operated at a much lower temperature (compared to the visbreaker stream preheated via E1 to E4) and has a longer residence time. The residue from this unit (tar) is cooled down by exchanging heat with the VBR stream in exchangers E5 to E9.

Laboratory tests conducted at the refinery identified the three chemical characteristics of the VBR and the tar stream in Table 1. CCR is the Conradson carbon residue, which is an indication of the quantity of coke that would form under thermal degradation conditions. The higher the CCR the more coking is expected in the furnace. The SHFT value (based on the Shell Hot Filtration Test method) is a measure of the portion of asphaltene that is insoluble in heavy oil at specific laboratory test conditions. The higher asphaltene content already present in the VBR stream is suspected to be the main cause of stream fouling. The products from the visbreaker process can also be unstable due to the presence of unsaturated olefins and di-olefins in the naphtha. These can react to form gums and non-volatile tar (Ancheyta, 2013).

During cleaning of exchangers E1 to E9, the refinery observed fouling on both the tube- and shell- sides of exchangers E1 to E4 and E6 to E9. Fouling on only the VBR stream was observed in E5.

The objective of the manuscript is to explore the possible fouling mechanisms and identify models to predict the fouling of thermal cracking units using an industrial case study.

Table 1: Chemical composition of the VB residue and Tar residue streams (source: German refinery).

Type	Visbreaker Residue	Tar
CCR	25 – 30 wt.%	43 – 50 wt.%
Asphaltenes	~ 16 wt.%	n.a.
SHFT	~ 0.08 wt.%	~ 5 wt.%

MODEL FORMULATION

The fouling models for heat exchangers associated with the thermal cracking unit are discussed in this section.

Heat transfer

The overall fouling resistance of the heat exchanger is presented as the sum of resistances in series:

$$\frac{1}{U} = \frac{1}{h_o} + R_{f,o} + \frac{d_o ln\left(\frac{d_o}{d_i}\right)}{2\lambda_w} + \frac{d_o}{d_i} R_{f,i} + \frac{d_o}{d_i}\frac{1}{h_i} \quad (1)$$

Here U is the overall heat transfer coefficient, h_o is the external film transfer coefficient and h_i is the internal film transfer coefficient, $R_{f,o}$ is the external fouling resistance, $R_{f,i}$ is the internal fouling resistance, λ_w is the wall thermal conductivity, d_i and d_o are the internal and external tube diameters, respectively. h_i is calculated for laminar, transient and turbulent flow using empirical correlations (ESDU, 1992, 2001). h_o is calculated based on a stream analysis method (ESDU, 1984).

Fouling mechanism

VR stream fouling

The VR stream, which is heated through exchangers E1 to E4 is assumed to experience a chemical reaction type fouling given by the equation:

$$\left(\frac{dR_f}{dt}\right)_{CRF} = \frac{c_1}{h} exp\left(\frac{-E_1}{RT_f}\right) - c_2\tau_s \quad (2)$$

Here, dR_f/dt is the fouling rate representing the rate of change in thermal resistance with time, c_1 is a deposition constant, c_2 is a removal constant, h is the film transfer coefficient, E_1 is the activation energy, R is the gas constant, T_f is the film temperature and τ_s is the surface shear stress. Subscript CRF denote, 'chemical reaction fouling'. Hong and Watkinson (2009) used a form of chemical reaction fouling model where an activation energy of 68 kJ mol^{-1} was used for heavy hydrocarbon/diluent blends. At this stage, the same activation energy value of 68 kJ mol^{-1} was used to fix E_1.

VBR and Tar stream fouling

VBR and Tar streams are liable to cause particulate depositions while being cooled through the heat exchangers due to their unstable composition (Table 1). The VBR stream is being heated through exchangers E5 to E9 after being cooled through exchangers E1 to E4. The VBR is assumed to cause particulate deposition also in the exchangers E5 to E9 and not chemical reaction fouling as the stream has already undergone thermal cracking in the visbreaking system at a temperature much higher than that exposed in the heat exchangers. Several mechanisms are involved in particulate fouling (Watkinson and Epstein, 1969):

- Transfer of foulant to the wall
- Adhesion of foulant to the solid surface
- Removal

Particulate fouling can be considered to involve deposition and removal (if conditions allow). The deposition term is modelled as:

$$\left(\frac{dR_f}{dt}\right)_{PF,deposition} = c_3\left(\frac{dm}{dt}\right)_{PF,deposition}$$

$$= c_3(N \times P) \quad (3)$$

Here, (dm/dt) is the particle mass deposition rate, N is the mean flux of particles to the wall and P is the probability of attachment. Subscript 'PF' denotes 'particulate fouling'. c_3 is a dimensional constant combining physical properties of the deposit. N is a function of the concentration of the particulates at the bulk, C_b, and the concentration of the particles at the surface, C_s.

$$N = k(C_B - C_S) \tag{4}$$

The mass transfer coefficient, k, is based on the theoretical analogy between heat, mass and momentum transfer (Metzner and Friend, 1958):

$$k = c_4 \frac{0.5C_f}{1.2 + 11.8\left(0.5C_f\right)^{0.5}(Sc-1)Sc^{-0.33}} \tag{5}$$

Here C_f is the friction factor, c_4 is a constant, and Sc is the Schmidt number given by:

$$Sc = \frac{\mu}{\rho D} \tag{6}$$

When $Sc \gg 1$, as is the case here, equation (5) can be simplified to:

$$k = c_5 \frac{\rho^{0.66} {C_f}^{0.5}}{\mu^{0.66}} \tag{7}$$

Here c_5 is a dimensional constant. As $C_B \gg C_S$, combining equations (4) and (7), and treating C_B as a fitting constant, gives:

$$N = c_6 \frac{\rho^{0.66} {C_f}^{0.5}}{\mu^{0.66}} \tag{8}$$

The probability of attachment can be a surface adhesion controlled process (Watkinson and Epstein, 1969) or can be a function of shear stress near the surface film (Yung et al., 1989). If the probability of attachment is dependent on a temperature dependent surface adhesion term, it is modelled by an Arrhenius type relation:

$$P = c_7 exp\left(-\frac{E_2}{RT_s}\right) \tag{9}$$

Combining equations (8) and (9), and including a deposit removal term the rate of particulate fouling (PF,1) is:

$$\left(\frac{dR_f}{dt}\right)_{PF,1} = c_8 \frac{\rho^{0.66} {C_f}^{0.5}}{\mu^{0.66}} exp\left(-\frac{E_2}{RT_s}\right) - c_9\tau_s \tag{10}$$

Here c_8 is a constant and $c_9\tau_s$ is a shear stress dependent removal term.

If the probability of attachment is not controlled by temperature dependent surface adhesion, but mass transfer, then the attachment is assumed to be a function of shear stress. In this case the rate of particulate fouling (PF,2) is presented as:

$$\left(\frac{dR_f}{dt}\right)_{PF,2} = \frac{c_{10}}{\mu^{0.66}} {\tau_s}^{-c_{11}} - c_{12}\tau_s \tag{11}$$

For heat exchangers E1 to E4 all the streams were in the turbulent flow regime. Chemical reaction fouling was taken to occur on the VR stream (shell-side) and particulate fouling on the VBR stream (tube-side). The overall fouling rate for heat exchangers E1 to E4 is given by either Model 1 or Model 2:

Model 1:

$$\left(\frac{dR_f}{dt}\right)_{Model\ 1} = \left(\frac{dR_f}{dt}\right)_{CRF} + \left(\frac{dR_f}{dt}\right)_{PF,1} \tag{12}$$

Model 2:

$$\left(\frac{dR_f}{dt}\right)_{Model\ 2} = \left(\frac{dR_f}{dt}\right)_{CRF} + \left(\frac{dR_f}{dt}\right)_{PF,2} \tag{13}$$

In exchangers E5 to E9 the fouling streams are all at laminar flow conditions. For heat exchanger E5, only particulate fouling is observed on the VBR stream (shell-side). In heat exchangers E6 to E9, both the VBR and tar stream undergo particulate fouling.

CASE STUDY

Fouling in the heat exchanger network associated with the thermal cracking units at the refinery (Fig. 1) is studied in this section. The thermo-physical properties of the streams are given in Table 2. The properties of VR stream can differ between refineries as this reflects the degree of fractional separation occurring in the vacuum column. The properties of VBR and tar streams can also vary between refineries as these depend on the degree of thermal cracking in the visbreaking systems.

Table 2: Stream thermo-physical properties at two temperatures. ρ, C_p, λ and μ denote density, specific heat capacity, thermal conductivity and dynamic viscosity, respectively.

Stream Name	Temperature	ρ	C_p	λ	μ
	°C	kg/m³	kJ/kg.K	W/m.K	cP
VBR	240	889	2.57	0.098	7.52
VBR	290	855	2.74	0.095	3.50
Tar	300	927	2.26	0.089	15.79
Tar	310	920	2.29	0.087	12.67
HGO	288	778	2.6	0.090	0.73
HGO	315	763	2.71	0.086	0.59
VR	160	931	2.35	0.104	93.79
VR	334	810	2.92	0.093	2.25

The temperature and volumetric flow measurements for a 1 year period were imported to the heat exchanger network model constructed in a commercial heat exchanger network simulator, SmartPM. Data reconciliation (Ishiyama et al., 2013) generated the exchanger operating conditions including, h, τ_s, T_s and C_f on both the shell- and tube-sides of the heat exchanger in addition to the overall performance data, including the exchanger duty, effectiveness, U and R_f. An example set of these parameters is given in the snapshot in Table 5.

Visbreaker unit (exchangers E1 to E4)

The inferred R_f profile is an overall fouling resistance value including the fouling resistances caused by fouling on both the tube-side and shell-side of the heat exchanger. The hollow circles in Fig. 2 show the fouling resistance profile obtained from data reconciliation for exchangers E1 to E4. The R_f profile in the first 100 days were ignored in the analysis as the noises introduced are believe to be caused by unstable operation of the visbreaker unit. The reconciliation indicated that both the shell- and the tube- sides of the exchangers operate under turbulent conditions. The R_f profile shows the hottest exchanger E4 exhibiting the highest fouling rate. The fouling rates in E1 to E4 range from 9.3×10^{-12} m^2 K J^{-1} to 4.6×10^{-11} m^2 K J^{-1}. Fouling was observed on both the shell-and tube-sides of the unit when the units were cleaned. The parameters for Model 1, equation (12)) were estimated to obtain the closest match for the observed fouling rates in E1 to E4. Table 4 lists the parameters that gave the best fit to the data.

The fitted parameters indicate that there is no removal on both the VR stream (undergoing chemical reaction fouling) and the VBR stream (undergoing particulate fouling). From Fig. 2(iv), Model 1 slightly over-predicts the fouling rate in E4. The activation energy for the particulate fouling model is low (< 10 kJ mol^{-1}). This implies, for this example, that the attachment process is governed by a physical process (mass transfer controlled) and not *via* a temperature dependent adhesion step.

Model 2 (equation (13)) is a modification of Model 1 (equation (12)), where the probability of attachment has been modified from a temperature dependent adhesion step to a simplified function of shear stress. The parameters for Model 2 were estimated to obtain the best fit for the observed plant fouling data in Fig. 2. The parameters are summarized in Table 4 (row Model 2). The fitted parameters again indicate no removal term and also no dependence of the shear stress. Model 2 slightly under-predicts the fouling rate for E1 (Fig. 2(i)).

Noise is rarely avoidable in refinery plant data. Therefore the accuracy of the fitted parameters is compromised through the reliability of the fouling resistance profiles. Advanced methodologies to obtain reliable R_f profiles, e.g. (Mirsadraee and Malayeri, 2015), could serve an important role to improve confidence in the fitted model parameters.

Table 3: Snapshot of operating conditions (at day 285) of heat exchangers E1 to E9 in Fig. 1.

	Cold stream							Hot stream						
	Inlet temperature	Outlet temperature	Mass flow rate	h	C_f	T_s	τ_s	Inlet temperature	Outlet temperature	Mass flow rate	h	C_f	T_s	τ_s
	°C	°C	kg s^{-1}	W m^{-2} K^{-1}	-	°C	Pa	°C	°C	kg s^{-1}	W m^{-2} K^{-1}	-	°C	Pa
E1	165	218	53	390	0.244	209	5.54	277	240	52	631	0.009	245	10.97
E2	218	261	53	478	0.113	252	2.02	309	277	52	839	0.008	284	9.85
E3	261	297	53	596	0.106	288	1.28	336	309	52	1041	0.007	316	9.16
E4	297	328	53	718	0.106	319	1.16	359	336	52	1213	0.007	343	8.70
E5	240	277	28	384	0.146	267	0.43	323	285	25	1432	0.006	301	3.69
E6	277	286	17	248	0.105	286	0.15	308	302	28	399	0.011	295	7.40
E7	286	295	17	259	0.105	295	0.14	302	295	28	549	0.010	303	6.99
E8	277	286	11	187	0.105	285	0.07	307	303	27	426	0.011	299	6.92
E9	286	293	11	194	0.105	292	0.07	303	299	27	521	0.011	303	6.77

Table 4: Best fit parameters for the fouling models used to predict fouling in the VR, VBR and Tar streams.

		Chemical reaction fouling			Particulate fouling 1			Particulate fouling 2		
		c_1	E_1	c_2	c_8	E_2	c_9	c_{10}	c_{11}	c_{12}
		h^{-1}	kJ mol^{-1}	m^{2}K J^{-1} Pa^{-1}	m^{2}K J^{-1} (Pa s)$^{0.66}$ (kg m^{-3})$^{-0.66}$	kJ mol^{-1}	m^{2}K J^{-1} Pa^{-1}	m^{2}K J^{-1} (Pa s)$^{0.66}$ (Pa)$^{-c11}$	-	m^{2}K J^{-1} Pa^{-1}
Model 1	VR stream	7.24	68	0	-	-	-	-	-	-
	VBR stream (turbulent flow)	-	-	-	3×10^{-11}	8	0	-	-	-
Model 2	VR stream	7.24	68	0	-	-	-	-	-	-
	VBR stream (turbulent flow)	-	-	-	-	-	-	7.33×10^{-13}	0	0
Model 3	VBR stream (laminar flow)	-	-	-	-	-	-	1.5×10^{-12}	0.5	0
	HGO stream	-	-	-	-	-	-	-	-	-
Model 4	VBR stream (laminar flow)	-	-	-	-	-	-	1.5×10^{-12}	0.5	0
	Tar stream (laminar flow)	-	-	-	-	-	-	2.0×10^{-10}	0.5	0

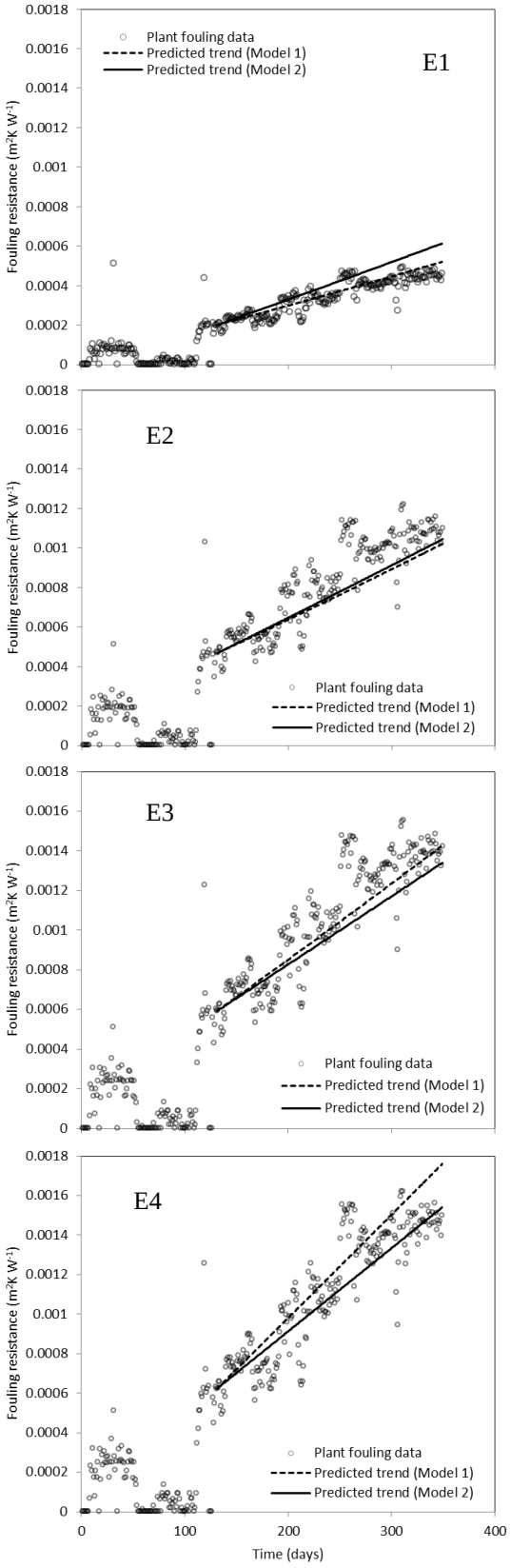

Fig. 2 Fouling resistance profiles for exchangers E1 to E4. Hollow circle = plant data; dashed and solid lines show predictions obtained by fitting Models 1 and 2, respectively.

Thermal cracking unit

The VBR streams and the tar streams in exchangers E5 to E9 (in Fig. 1) experience severe fouling which is seen when the exchangers are taken offline for cleaning. All fouling streams are operated under laminar flow conditions (Re < 2500), due to the high stream viscosities and pressure drop constraints.

E5 has fouling only on the VBR stream. If the particulate fouling parameters obtained in Model 1 or Model 2 (Table 4) were used to predict fouling in E5, the actual fouling rate is under predicted (dashed line and bold solid line in Fig. 3).

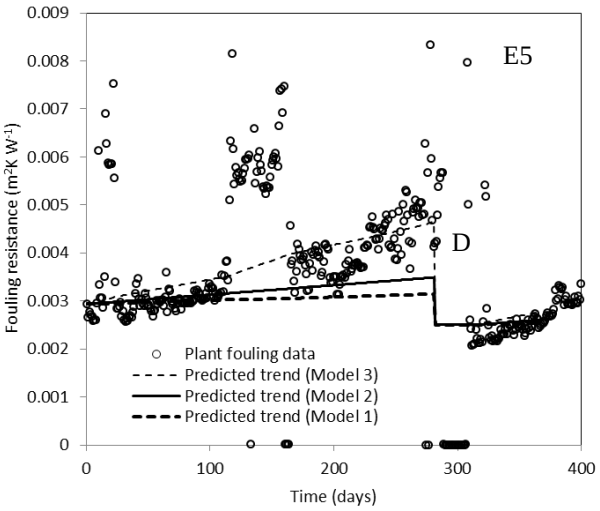

Fig. 3 Fouling resistance profile for exchanger E5. Hollow circle = plant data; solid dashed line = Model 1, solid line = Model 2 and dashed line = Model 3. Resistance drop at 'D' indicates start of a cleaning action.

The under-prediction is likely due to be the change in flow regime of the VBR stream from turbulent to laminar when flowing from E1-E4 to E5. Model 3 was used to refit the particulate fouling model parameters for the E5 exchanger:

$$\left(\frac{dR_f}{dt}\right)_{Model\ 3} = \left(\frac{dR_f}{dt}\right)_{PF,2} \tag{14}$$

The parameters (model 3, Table 4) now indicate a dependence on shear stress but no removal.

The R_f profiles for exchangers E6 to E9 are shown in Fig. 4. The exchangers are cleaned several time during the period considered. The cleaning actions are marked 'D'. There is significant scatter in plant data relating to the period when the exchanger was taken offline for cleaning or when the exchanger was back online after cleaning. E6 to E9 exhibit extremely high fouling rates (much larger than in E1 to E5).

The particulate fouling model given by equation (11) is assumed to apply to both the shell- and tube- sides of the exchangers E6 to E9. The overall fouling rate for exchangers E6 to E9 is given via:

$$\left(\frac{dR_f}{dt}\right)_{Model\ 4} = \left(\frac{dR_f}{dt}\right)_{PF,2\ (VBR)} + \left(\frac{dR_f}{dt}\right)_{PF,2\ (TAR)} \tag{15}$$

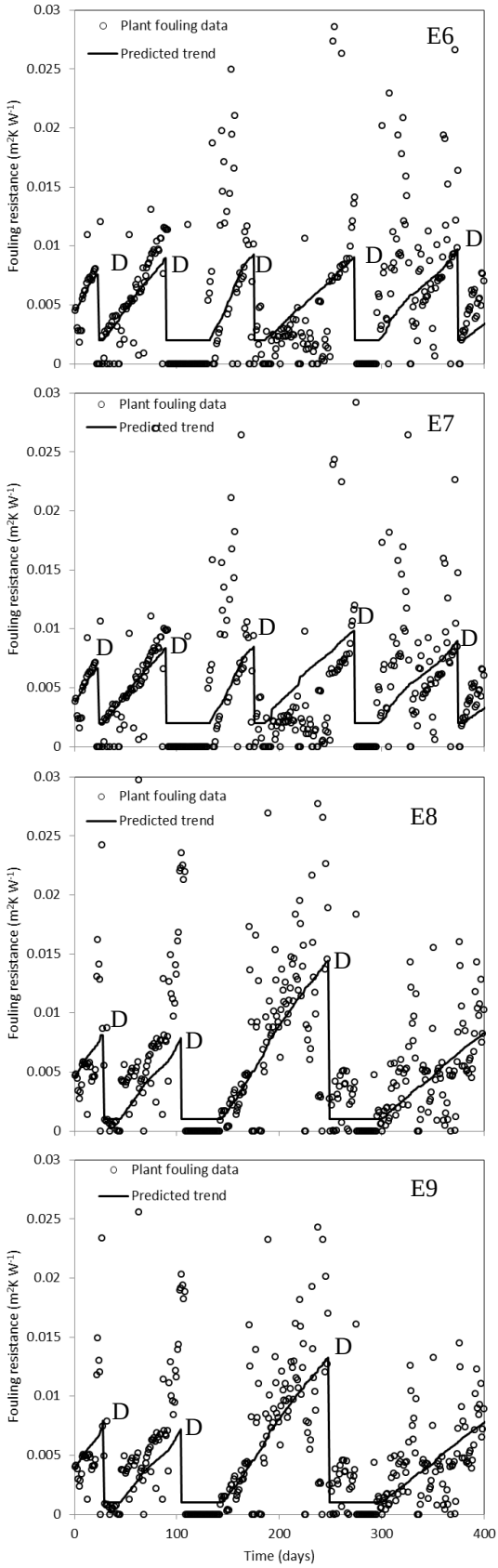

Fig. 4 Fouling resistance profiles for exchangers E6 to E9. Hollow circle = plant data; solid line shows prediction with Model 4. Resistance drop at 'D' indicates start of a cleaning action.

The fouling model parameters for the VBR stream are the same as those obtained in Model 3 (Table 1). The fitted parameters for the tar stream (Model 4, Table 1), indicate no deposit removal. The index (0.5) of the shear stress in the probability of attachment is equal to that obtained for the VBR stream.

DISCUSSION

The fouling contributions predicted *via* each stream are summarized in Table 5. Based on the fitted model, significant fouling is observed for the hot stream where particulate deposition occurs. This is consistent with the observed tube-side fouling during heat exchanger cleaning of the system. The fouling model parameters giving the best fit to the plant data are summarized in Table 4.

Table 5: Average predicted fouling rates for the cold stream, hot stream and overall exchanger. The associated particulate fouling model is based on equation (11).

	Predicted average fouling rate over the data range		
	Cold stream	Hot Stream	Total fouling rate
	$m^2K\ J^{-1}$	$m^2K\ J^{-1}$	$m^2K\ J^{-1}$
E1	2.48E-13	1.17E-11	1.20E-11
E2	7.77E-13	2.83E-11	2.91E-11
E3	1.68E-12	3.66E-11	3.83E-11
E4	2.96E-12	3.76E-11	4.05E-11
E5	2.16E-11	-	2.16E-11
E6	2.70E-11	1.44E-09	1.47E-09
E7	2.99E-11	1.61E-09	1.64E-09
E8	2.69E-11	1.12E-09	1.15E-09
E9	2.93E-11	1.22E-09	1.25E-09

Formulation of Equation (7) had included the mass diffusivity as a fitting parameter (included as part of constant C_5). For situation where the stream has a low asphaltene content, the mass diffusivity could be approximated from the Wilke and Chang correlation (Wilke and Chang, 1955):

$$D = c_{13}\frac{T_S}{\mu} \tag{16}$$

In this case equation (10) is modified to:

$$\left(\frac{dR_f}{dt}\right)_{PF,3} = c_{14}\frac{{T_S}^{0.66}\rho^{0.66}{C_f}^{0.5}}{\mu^{4/3}}exp\left(-\frac{E_3}{RT_s}\right) - c_{15}\tau_s \tag{17}$$

and equation (11) becomes

$$\left(\frac{dR_f}{dt}\right)_{PF,4} = c_{16}\frac{{T_S}^{0.66}\rho^{0.66}}{\mu^{4/3}}{\tau_s}^{-c_{17}} - c_{18}\tau_s \tag{18}$$

The overall fouling rate could be then written as Model 5 or Model 6.

$$\text{Model 5: } \left(\frac{dR_f}{dt}\right)_{Model\ 5} = \left(\frac{dR_f}{dt}\right)_{CRF} + \left(\frac{dR_f}{dt}\right)_{PF,3} \tag{19}$$

$$\text{Model 6: } \left(\frac{dR_f}{dt}\right)_{Model\ 6} = \left(\frac{dR_f}{dt}\right)_{CRF} + \left(\frac{dR_f}{dt}\right)_{PF,4} \tag{20}$$

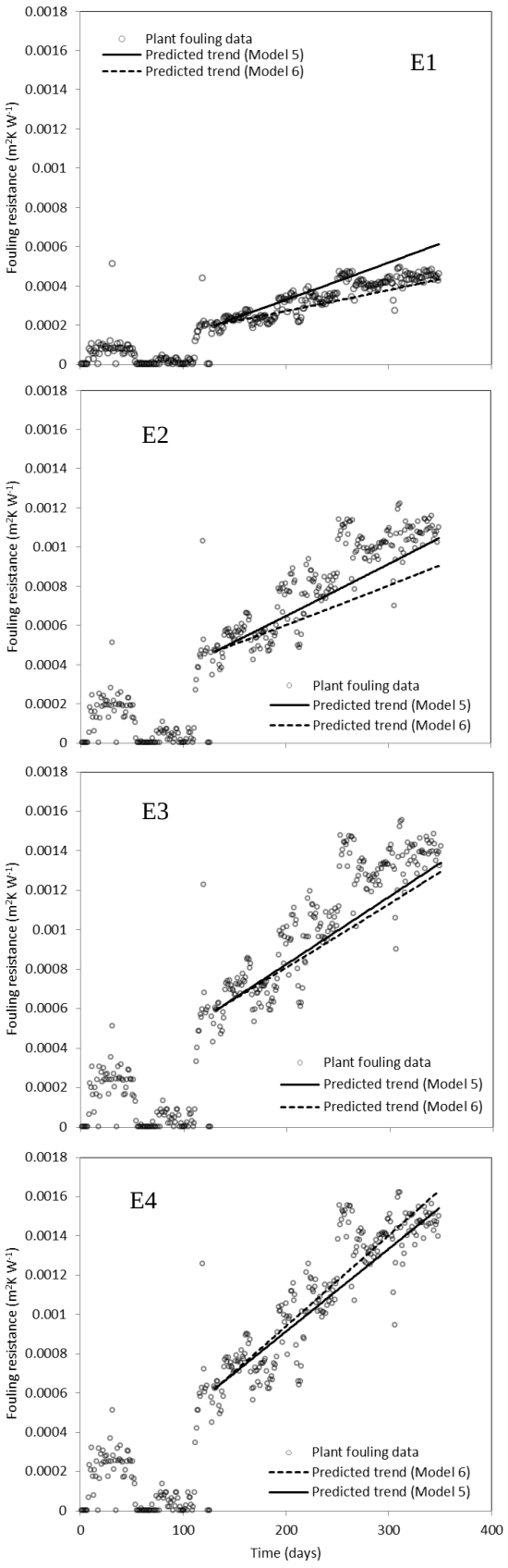

Fig. 5 Fouling resistance profiles for exchangers E1 to E4. Hollow circle = plant data; solid and dashed lines show predictions *via* Models 5 and 6, respectively.

For the VBR stream, the reported average asphaltene content is relatively high (~16 wt%, Table 1). However, the SHFT results in Table 1 show that the insoluble asphaltene content under specific test condition is ~ 0.06 wt%. This implies a considerable amount of asphaltenes could be soluble under laboratory conditions. If this was the case in practical operation, Models 5 or 6 could result in a better fit compared to Models 1 or 2. Equations (17) and (18) were fitted to the exchanger profiles of E1 to E4 (Fig. 5). The best fit parameters obtained are summarized in

Table 7.

The parameter fitting indicates that Model 5 over-predicts the fouling rate for E1 and under predicts for E2 and E3. Model 6 under-predicts fouling in exchangers E2 and E3. The R^2 values (summarized in Table 6) indicate that Model 2 gives the best fit to the plant data.

Table 6: Comparison of R^2 value for Models 1, 2, 5 and 6 (based on analysis of exchangers E1 to E4).

Fouling model	R^2
Model 1	0.66
Model 2	0.88
Model 5	0.65
Model 6	0.71

The fouling models discussed here can now be used for predictive studies to optimize energy recovery.

CONCLUSIONS

1. Plant fouling data for heat exchangers in thermal cracking units were extracted.
2. The fouling mechanisms were identified as chemical reaction fouling mechanism on the vacuum residue stream and particulate fouling mechanism on the visbreaker residue and tar streams.
3. The overall fouling resistance of a heat exchanger can be separated into the fouling resistance contributions of the shell-side and tube-side fouling deposits if the dynamic fouling behaviour of shell- and tube-sides are modelled.
4. New fouling models were incorporated in IHS SmartPM software for use in ongoing plant energy efficiency studies, including heat exchanger cleaning scheduling.

NOMENCLATURE

c_1 dimensional constant, s^{-1}
c_2 dimensional constant, $m^2\,K\,J^{-1}\,Pa^{-1}$
c_3 dimensional constant, $m^2\,K\,J^{-1}\,(s\,kg^{-1})$
c_4 dimensional constant, $m\,s^{-1}$
c_5 dimensional constant, $m\,s^{-1}\,(Pa\,s\,m^3\,kg^{-1})^{0.66}$
c_6 dimensional constant, $kg\,m^{-2}\,s^{-1}$
c_7 dimensional constant, -
c_8 dimensional constant, $m^2K\,J^{-1}\,(Pa\,s\,m^3\,kg^{-1})^{0.66}$
c_9 dimensional constant, $m^2K\,J^{-1}\,Pa^{-1}$
c_{10} dimensional constant, $m^2K\,J^{-1}\,(Pa\,s)^{0.66}\,(Pa)^{C11}$
c_{11} dimensional constant, -
c_{12} dimensional constant, $m^2K\,J^{-1}\,Pa^{-1}$
c_{13} dimensional constant, $m^2Pa\,K^{-1}$
c_{14} dimensional constant, $m^2KJ^{-1}K^{-0.66}(kg\,m^{-3})^{-0.66}(Pas)^{4/3}$

c_{15} dimensional constant, $m^2K\ J^{-1}\ Pa^{-1}$
c_{16} dimensional constant, $m^2K\ J^{-1}\ K^{-1}(kg\ m^{-3})^{-0.66}\ (Pa\ s)^{4/3}\ (Pa)^{C17}$
c_{17} dimensional constant, -
c_{18} dimensional constant, $m^2K\ J^{-1}\ Pa^{-1}$
C_B concentration of particle at bulk fluid, $kg\ m^{-3}$
C_f fanning friction factor, -
C_S concentration of particle at surface, $kg\ m^{-3}$
C_p specific heat capacity, $J\ kg^{-1}\ K^{-1}$
d tube diameter, m
D mass diffusivity, $m^2\ s^{-1}$
E_1 activation energy (chemical reaction), $J\ mol^{-1}$
E_2 activation energy (particle adhesion), $J\ mol^{-1}$
E_3 activation energy (particle adhesion), $J\ mol^{-1}$
h film transfer coefficient, $W\ m^{-2}\ K^{-1}$
k mass transfer coefficient, $m\ s^{-1}$
m mass flow rate, $kg\ s^{-1}$
N mean mass flux, $kg\ m^{-2}\ s^{-1}$
P probability of attachment, -
Pr Prandtl number, –
R gas constant, $J\ mol^{-1}\ K^{-1}$
R_f fouling resistance, $m^2K\ W^{-1}$
R_w wall resistance, $m^2K\ W^{-1}$
Re Reynolds number, –
Sc Schmidt number, –
T_f film temperature, K
T_s surface temperature, K
U overall transfer coefficient, $W\ m^{-2}\ K^{-1}$

Subscripts
i internal
o external
w wall

Greek symbols
λ thermal conductivity, $W\ m^{-1}\ K^{-1}$
μ dynamic viscosity, Pa s
ρ density, $kg\ m^{-3}$; τ_s surface shear stress, Pa

Acronyms
CCR Conradson Carbon Number;
CRF chemical reaction fouling
PF particulate fouling
SHFT Shell Hot Filtration Test
VB visbreaker
VBR visbreaker residue;
VR vacuum residue

REFERENCES

Ancheyta, J. (2013). Modeling of processes and reactors for upgrading of heavy petroleum (CRC Press).

ESDU (1984). Baffled shell-and-tube heat exchangers: flow distribution, pressure drop and heat transfer coefficient on the shellside (London, UK: IHS).

ESDU (1992). Forced convection heat transfer in straight tubes. Part 1: turbulent flow (London, UK: IHS).

ESDU (2001). Forced convection heat transfer in straight tubes Part 2. laminar and transitional flow (London, UK: IHS).

Hong, E., and Watkinson, A.P. (2009). Precipitation and fouling in heavy oil-diluent blends. Heat Transf. Eng. *30*, 786–793.

Ishiyama, E.M., Pugh, S.J., Kennedy, J., Wilson, D.I., Ogden-Quin, A., and Birch, G. (2013). An industrial case study on retrofitting heat exchangers and revamping preheat trains subject to fouling. In Heat Exchanger Fouling and Cleaning, (Budapest, Hungary),.

Melo, L.F., and Pinheiro, J.D. (1984). Hydrocynamics effects on particulate fouling. In First U.K. National Conference on Heat Transfer, (Pergamon), pp. 381–390.

Metzner, A.B., and Friend, W.L. (1958). Theoretical analogies between heat, mass and momentum transfer and modifications for fluids of high Prandtl or Schmidt numbers. Can. J. Chem. Eng. *36*, 235–240.

Mirsadraee, A., and Malayeri, M.R. (2015). Analysis of highly noisy crude oil fouling data using kalman filter. In Heat Exchanger Fouling and Cleaning, (Enfield, Dublin),.

Mueller-Steinhagen, H., and Bloechl, R. (1988). Particulate fouling in heat exchangers. In Proceedings - IPENZ Annual Conference, (New Plymouth, NZ), pp. 275–287.

Mueller-Steinhagen, H., Reif, F., Epstein, N., and Watkinson, A.P. (1988). Influence of operating conditions on particulate fouling. Can. J. Chem. Eng. *66*, 42–50.

Vašak, F., Kaštánek, F., Bowen, B.D., Chen, C.Y., and Epstein, N. (1995). Fine particle deposition in laminar and turbulent flows. Can. J. Chem. Eng. *73*, 785–792.

Watkinson, A.P., and Epstein, N. (1969). Gas oil fouling in a sensible heat exchanger. Chem Eng Prog Sym Ser *65*, 84–90.

Wilke, C.R., and Chang, P. (1955). Correlation of diffusion coefficients in dilute solutions. AIChE J. *1*, 264–270.

Yung, B.P.K., Merry, H., and Bott, T.R. (1989). The role of turbulent bursts in particle re-entrainment in aqueous systems. Chem. Eng. Sci. *44*, 873–882.

Table 7: Best fit parameters for the fouling models used to predict fouling in the VBR stream in the visbreaking system.

		Chemical reaction fouling			Particulate fouling 3			Particulate fouling 4		
		c_1	E_1	c_2	c_{14}	E_3	c_{15}	c_{16}	c_{17}	c_{18}
		h^{-1}	$kJ\ mol^{-1}$	$m^2K\ J^{-1}\ Pa^{-1}$	$m^2K\ J^{-1}\ K^{-0.66}(Pa\ s)^{(4/3)}\ (kg\ m^{-3})^{-0.66}$	$kJ\ mol^{-1}$	$m^2K\ J^{-1}\ Pa^{-1}$	$m^2K\ J^{-1}\ (Pa\ s)^{0.66}\ (Pa)^{-c11}$	-	$m^2K\ J^{-1}\ Pa^{-1}$
Model 5	VR stream	7.24	68	0	-	-	-	-	-	-
	VBR stream (turbulent flow)	-	-	-	2.51×10^{-16}	10	0	-	-	-
Model 6	VR stream	7.24	68	0	-	-	-	-	-	-
	VBR stream (turbulent flow)	-	-	-	-	-	-	2.47×10^{-17}	0	0